CHAPTER III

Assessments of The Living Drug-Sensitive and -Resistant Cells Response to Artemisinin, Artesunate and Dihydro-artemisinin by ^{1}H-NMR Spectroscopy

Submitted

Journal of Magnetic Resonance

Assessments of The Living Drug-Sensitive and -Resistant Cells Response to Artemisinin, Artesunate and Dihydroartemisinin by ^{1}H-NMR Spectroscopy

Paiboon Reungpatthanaphong[1], Suchart Kothan[1], Raweewan Kanpairhoa[1], Laurence le Moyec[2], Samlee Mankhetkorn[1]*

[1]Laboratory of Physical Chemistry, Molecular and Cellular Biology, Department of Radiologic Technology, Faculty of Associated Medical Sciences, Chiang Mai University 50200, Thailand
[2]Laboratoire LPBC-CSSB, UMR CNRS 7033, Université Paris 13, 74 avenue, Marcel Cachin, 93017 Bobigny Cedex

Abstract

Artemisinin and its derivative efficiently exhibited anticancer activities at both *in vitro* and *in vivo*, but no reports deal with the possibility of their modes of actions. In this study, we sought to investigate the response to artemisinin, artesunate and dihydroartemisinin of K562, GLC4, K562/*adr* with overexpressing P–glycoprotein and GlC4/*adr* with overexpressing MRP1 protein using ^{1}H–NMR spectroscopy which is powerful tool allows to simultaneously monitoring of the metabolic biomarkers. Before treatment, the drug-sensitive cells produce energy supplies via oxidative metabolism, while an up–regulation of glycolysis that become dominate in the drug–resistant cells. After treatment, the drugs inhibit the oxidative metabolism of K562 but not of GLC4 cells, inhibit the anaerobic and stimulate the oxidative metabolism of the MDR cells. An abnormal oxidative metabolism was observed in K562/adr cells; as a decrease in glutamate is not accompanied by any increase in aspartate. The change in metabolic pattern was accompanied by an intracellular acidification and an induction of both necrosis and apoptosis. ^{1}H–NMR spectroscopy is suitable technique for studying the cellular response to cytotoxic drugs.

Keywords: Qinghaosu, anticancer, Multidrug resistance (MDR) phenomenon, metabolic biomarkers, ^{1}H–NMR spectroscopy, acridine orange

*Corresponding Author:

Samlee Mankhetkorn, Ph.D.
Laboratory of Physical Chemistry, Molecular and Cellular Biology,
Department of Radiologic Technology,
Faculty of Associated Medical Sciences,
Chiang Mai University 50200, Thailand
Telephone: 66-053-949305
Fax: 66-053-946024 E-mail: samlee@chiangmai.ac.th

1. INTRODUCTION

Artemisinin and its derivatives such as artesunate and dihydroarte-misinin, a new generation of antimalarial drugs with low toxicity (Klayman, 1985; Benakis *et al.*, 1997; Hien *et al.*, 1993) are considered as potent anticancer agents (Singh *et al.*, 2002; Singh *et al.*, 2001; Efferth *et al.*, 2001; Efferth *et al.*, 2002; Woerdenbag *et al.*, 1993) particularly for overcoming MDR phenomena (Reungpatthanaphong & Mankhetkorn, 2002). Furthermore, it was reported that artemisinin and its derivatives also exhibited anti-angiogenic and apoptosis-inducing activity against endothelial cells *in vitro* studies (Chen *et al.*, 2004). Nevertheless, the multiple mechanisms of its cytotoxicity have not been fully clarified.

We have previously reported that artemisinin, artesunate and dihydroarte-misinin poorly inhibited P–glycoprotein and did not inhibit MRP1 protein function in multidrug resistant K562/*adr* cells, overexpression P–glycoprotein, or in GLC4/*adr* cells overexpression of MRP1-protein, respectively. However, they increased in cytotoxic effect induced by pirarubicin or doxorubicin only in MDR cell lines. We also demonstrated that these qinghaosu modulate mitochondrial function, leading to a decrease in intracellular ATP content in K562, K562/*adr*, GLC4 and GLC4/*adr* cells (Reungpatthanaphong & Mankhetkorn, 2002), suggesting that the drugs might alter the cellular metabolism.

Recently, it was demonstrated that cancer cells exhibit an abnormal energy metabolism compared with normal mammalian cells which derive most of their energy supplies from oxidative phosphorylation. The catabolism of glucose through glycolysis produces pyruvate that can be converted to lactate in a reaction catalysed by lactate dehydrogenase or to alanine in a reaction catalysed by alanine aminotransferase. Under non-oxygen limiting conditions, oxidative metabolism dominates, and pyruvate enters the tricarboxylic acid (TCA) cycle through the action of enzymes pyruvate dehydrogenase and pyruvate carboxylase. The α–ketoglutarate and malate generated by TCA cycle are in equilibrium with the glutamate and aspartate pool, respectively (Papas *et al.*, 2001). These metabolic products such as lactate, alanine, glutamate, aspartate etc... can be used as biomarkers for the non–invasive monitoring of cellular response to cytotoxic drugs (Papas *et al.*, 2001; Sunil *et al.*, 2006). In fact these biomarkers were studied in cell culture system and *in vivo* using ^{1}H–NMR spectroscopy. Both *in vivo* magnetic resonance spectroscopy (MRS) and high–resolution solution state techniques allow to simultaneously monitoring these aqueous and lipid–soluble metabolites (Pfeuffer *et al.*, 2005; Miccheli *et al.*, 2005; Sharma *et al.*, 2004). Most ^{1}H–NMR investigations have focused on detecting changes of the methyl signals of, N-acetylaspartate, total creatine (creatine and phoshocreatine), choline, lactate, glutamate, alanine, aspartate and myo-inositol (Pfeuffer *et al.*, 1999). The ratios of glutamate/lactate and aspartate/lactate before and after treatment can be used as biomarkers for anaerobic and oxidative metabolism, respectively. (Sunil, In Press: 2006).

In this study, the metabolic changes of drug-sensitive and drug–resistant cells provoke by exposing to artemisinin, artesunate or dihydro-artemisinin was investigated by using ^{1}H–NMR spectroscopy. The biological effects such as apoptosis, necrosis and the change in cytoplasmic environments affected by the drugs were confirmed by flow cytometry. We demonstrate that artemisinin, artesunate and dihydro-artemisinin induced metabolic phenotypic changes in K562, K562/*adr*, GLC4 and GLC4/*adr* cells. The oxidative metabolic dominated in untreated drug–sensitive cell lines and a considerably enhancement of anaerobic metabolic was up to ≈ 55 ± 2 % in drug-resistant cells. The drugs decrease in oxidative metabolic of both drug-sensitive cells while increase in the efficacy of oxidative metabolic of both drug-resistant cells lines. These were accompanied by an intracellular acidification and an induction of apoptosis and necrosis.

2. Materials and Methods

2.1 Drugs and Chemicals

Acridine orange and tetrazolium salt MTT were from Amresco. Artemisinin and D_2O were from Sigma. Artesunate was kindly provided by Professor Ruchanee Udomsangpetch, Faculty of Science, Mahidol University, Thailand. Dihydroartemisinin was synthesized and provided by Professor Yodhathai Thebtaranonth, Department of Chemistry, Faculty of Science, Mahidol University, Thailand. Purified pirarubicin (4-Q-tetrahydropyrayl-doxorubicin) was kindly provided by laboratoire Roger Bellon (France). Deionized double distilled water was used throughout the experiments for solutions and buffers. Experiments were performed at 37 °C using a HEPES–Na^+ medium consisting of 132 mM NaCl, 3.5 mM KCl, 1 mM $CaCl_2$, 0.5 mM $MgCl_2$, 5 mM glucose, 20 mM HEPES, pH 7.25. A stock solution of 0.012 M MTT was prepared in HEPESNa1 buffered solution, filtered through a 0.22 μm filter, and stored at 4 °C. Solutions of qinghaosu and pirarubicin were freshly prepared before being used. The concentration of anthracyclines was spectrophotometrically determined using ε at 480 nm equal to 11,500 $M^{-1} \cdot cm^{-1}$ (Shimadzu UV2501–PC).

2.2 Cell lines, cell culture and cytotoxicity assay

The K562 human erythromyelogenous leukemic cell line and its DOX–resistant, P–glycoprotein–overexpressing K562/*adr* subline (Lozio *et al.*, 1975; Tsuro,1986) and the GLC4 human small cell lung carcinoma cell line and its DOX–resistant, MRP1–overexpressing GLC4/*adr* subline (Muller *et al.*, 1994; Versantvoort *et al.*, 1995) were routinely cultured in RPMI 1640 medium supplemented with 10% (v/v) fetal calf serum (GIBCO BRL, USA) in a humidified atmosphere of 95% air and 5% CO_2 at 37 °C. For the assays, cell cultures were initiated at a density of 5×10^5 cells/ml to have cells in the exponential growth phase; the cells were used 24 h later when the culture had grown to about 8×10^5 cells/ml. Cell viability was assessed by trypan blue exclusion. The number of cells was determined with a hemo-cytometer.

The cytotoxicity assay was performed as follows. Cells (5×10^4 cells/mL) were incubated in the presence of various drug concentrations. The viability of cells was then determined using the MTT assay based on the reduction of MTT to

purple-colored formazan by live, but not dead, cells. The concentration of drug required to inhibit cell growth by 50% when measured at 72 h (IC_{50}) was determined by plotting the percentage of cell growth inhibition versus the drug concentration. The resistance factor (RF) was defined as the IC_{50} of resistant cells divided by the IC_{50} of the corresponding sensitive cells (Mankhetkorn *et al.*, 1996). Under our experimental conditions, the IC_{50} values were 10 ± 2 nM for K562 and GLC4 cells. The RF values were 40 and 7 for K562/*adr* and GLC4/*adr* cells, respectively.

2.3 Induction of apoptosis

For induction of the apoptosis assay, exponentially growing cells were seeded in six-well plates at initial density at 1×10^5 with 5 ml medium. After 24 h, varied concentrations of compounds (artemisnin & derivatives) ranging from 0 to 50 µM were added and the cells were further incubated at 37 °C for various times: 6, 24 and 72 h. Quercetine concentrations ranging from 2.5 to 20 µM were used as a positive control to induce apoptosis (Kothan *et al.*, 2004).

2.4 Cytofluorometric staining of the cells.

Cells (1×10^6) were taken for detection of apoptosis and centrifuged for 5 min, 1000×g at room temperature (25 °C), resuspended and washed once with 5 mL phosphate–buffered saline prior to be stained with Annexin V (apoptosis detection kit from R&D Systems). Flow cytometry analysis was performed in a Coulter Epics XL–MCL™ (Beckman Coulter, Miami, U.S.A.) and cells were evaluated on 5000 events per sample. Biparametric histograms were used to visualise the distribution of cells as a function of their signal intensity with respect to Annexin V–FITC and PI.

2.5 NMR analysis

Cells were washed twice in 1 mL PBS 150 mM, twice in PBS/D_2O, centrifuged at 250×g and counted. Then, 10^7 cells were resuspended in 400 µL PBS/D_2O before transfer to a 5-mm Shigemi NMR tube. Experiments were performed without rotation, and the analysed cell pellet was maintained in the coil volume in the Shigemi NMR tube. The NMR proton spectra of whole cells were obtained at 25°C on a Unity Inova spectrometer (Varian, France) working at 500 MHz. One–dimensional runs were performed by accumulating 128 transients of 90° pulse with 2 s relaxation time. The signal from the residual water was suppressed by the presaturation technique, by using 0.03 mW irradiation for 2 s. The acquisition time was 1.34 s on 16K data points, corresponding to a spectral width of 6 kHz. The Fourier transform was applied without zero–filling using an exponential window multiplication function corresponding to 1 Hz line broadening. The resonances were integrated after automatic baseline correction. Two-dimensional COSY runs were performed with 2K data points in the F2 direction and 256 data points in the F1 direction. The two-dimensional Fourier transformation was applied after zero filling to 512 data points in the F1 direction with a sine-bell function in both directions. Each run consisted of a one-dimensional acquisition and a two–dimensional COSY spectrum. Peak assignments were based on data from the literature (Pfeuffer *et al.*, 1999; Mannechez *et al.*, 2005). The peak areas were measured by manual integration with the Bruker WINNMR software using a manual tangential baseline correction for each

peak, and the assigned peak areas were normalized to the creatine peak area. The following resonances were integrated: methyl group (CH_3 at 0.9 ppm), methylene group (CH_2 at 1.3 ppm), choline N-trimethyl group ($N+(CH_3)_3$ at 3.2 ppm) and creatine (CH_3 at 3.05 ppm). The values obtained for the different treatments of the cells lines were compared by ANOVA analysis followed by a Student–Neumann–Keuls test for group-to-group comparison. $P < 0.05$ was considered as a significant value.

The possible contribution of lactate to the 1.3 ppm signal was eliminated by analysing 2D Cosy spectra in whole cells, which resolved the resonances of lactate from fatty acid chains. In fixed cells, we calculated the ratio of the double-bond signal (CH = CH at 5.4 ppm) to CH_2 peak area. As both groups belong to fatty acyl chains, this ratio remained constant since lactate did not significantly contribute to the increase of the CH_2 signal.

2.6 Flow cytofluorometric determination of cellular acridine orange uptake

Cells (1×10^6) were centrifuged for 5 min, 1000×g at room temperature (25 °C), resuspended and washed once with 5 mL phosphate-buffered saline prior to an further incubation in the presence of 1 μM acridine orange for 30 minutes. Flow cytometry analysis was performed in a Coulter Epics XL–MCL™ (Beckman Coulter, Miami, U.S.A.) and cells were evaluated on 5000 events per sample. Biparametric histograms were used to visualise cells distributed as a function of their signal intensity with respect to red and green fluorescence.

Statistical analyses

The results are presented as means ± SD. Multiple statistical comparisons were performed using the T–tests analysis.

3. RESULTS

3.1. ^{1}H-NMR spectra

The ^{1}H-NMR spectra obtained from K562, K562/*adr*, GLC4 and GLC4/*adr* cells were shown in Figure 1. The ^{1}H–NMR spectra revealed differences in lactate (δ = 1.33, 4.11 ppm), alanine (δ = 1.47 ppm), *N*–acetylaspartate (δ = 2 ppm) and glutamate (δ = 3.7, 2.35 ppm). The resonance peaks of taurine (δ = 3.42 ppm) and myo–inositol (δ = 3.5 ppm) were also assigned in spectra of the cell lines. The alanine resonance peak represented as the characteristic of ^{1}H-NMR spectra of K562 and K562/*adr* since the peak was not found in those obtained from GLC4 and GLC4/*adr* cells.

a)^{1}H–NMR spectra of untreated cells: the metabolites products of drug–sensitive and drug–resistant cells before treatment were analyzed as indicated in Table 1. The signal surfaces measured of glutamate resonance was found 2.61 ± 0.8 fold for K562 and 1.31 ± 0.16 fold for GLC4 cells higher than lactate. GLC4 cells produce two-fold lactate higher than K562 cells (P<0.01). The ratios of glutamate to lactate was equal to 0.74 ± 0.14 for K562/adr and 0.73 ± 0.03 for GLC4 cells where no–significant difference of lactate was found in both MDR cells (lactate = 0.59 ± 0.17 for K562/adr and 0.68 ± 0.15 for GLC4/adr, P<0.56). Both drug–resistant cells significantly produce lactate higher than K562 cells ($P <$ 0.01) but no-significant difference to GLC4 ($P < 0.16$).

Table 1. NMR signals integration reported to creatine peak integration measured on K562, GLC4, K562/*adr* and GlC4/*adr* spectra. Cells (10^6 cell/mL for 10 mL) were incubated in the absence or in the presence of 30 μM drugs for 2 h at 37 °C, centrifuge at 1800 rpm for 10 minutes. The pellets were rinsed twice using PBS and three times washed using PBS/D_2O. The cells were counted using hematocytometer and were loaded into a 5–mm Shigemi NMR tube, completed with 450 mL PBS/D_2O.

Metabolite	K562				K562*adr*				GLC4				GLC4*adr*			
	-	ART	ARTS	DHA	-	ART	ARTS	DHA	-	ART	ARTS	DHA	-	ART	ARTS	DHA
Taurine	0.26 ±0.02	0.23 ±0.02	0.19 ±0.04	0.29 ±0.01	0.36 ±0.08	0.22 ±0.07	0.23 ±0.04	0.35 ±0.04	0.51 ±0.17	0.89 ±0.12	0.74 ±0.03	0.72 ±0.4	0.32 ±0.02	0.78 ±0.4	0.32 ±0.02	0.34 ±0.09
Lactate	0.27 ±0.05	0.30 ±0.07	0.20 ±0.06	0.26 ±0.02	0.59 ±0.17	0.30* ±0.03	0.28** ±0.12	0.33* ±0.03	0.45 ±0.05	0.41 ±0.03	0.32 ±0.11	0.90 ±0.68	0.68 ±0.15	0.32** ±0.04	0.33** ±0.11	0.25** ±0.06
Glutamate	0.49 ±0.18	0.25** ±0.02	0.24** ±0.02	0.23*** ±0.01	0.50 ±0.14	0.27** ±0.02	0.29** ±0.05	0.31*** ±0.09	0.59 ±0.01	0.44 ±0.23	0.47 ±0.07	0.78 ±0.61	0.50 ±0.09	0.47 ±0.09	0.49 ±0.16	0.43 ±0.15
Aspartate	0.14 ±0.11	0.09 ±0.03	0.11 ±0.04	0.55* ±0.01	0.31 ±0.03	0.30 ±0.1	0.28 ±0.01	0.37 ±0.13	1.21 ±0.4	1.05 ±0.11	0.76 ±0.19	1.38 ±0.12	0.73 ±0	1.21* ±0.09	1.05** ±0.13	0.96* ±0.04
myo-Inositol	1.25 ±0.26	0.93 ±0.32	0.56** ±0.02	1.00 ±0.01	1.27 ±0.18	0.61* ±0.08	0.61* ±0.12	1.13 ±0.11	0.92 0.03	0.59* ±0.02	0.36* ±0.05	0.88 ±0.35	0.69 ±0.02	0.78 ±0.4	0.80 ±0.07	0.73 ±0.09

Presented are mean values and their standard deviations (SD) for each cell line and each qinghaosu after 2h treatment. The effects of treatments on K562, GLC4, K562/*adr* and GlC4/*adr*cells were compared to control untreated cells by independent t–test.

* significantly different from control , $P < 0.05$

** significantly different from control, $P < 0.10$

*** significantly different from control, $P < 0.15$

Table 2. NMR peak ratios measured on K562, GLC4, K562/*adr* and GlC4/*adr* spectra obtained from the series of experiments described in the table 1.

Metabolite	K562				K562*adr*				GLC4				GLC4*adr*			
	-	ART	ARTS	DHA	-	ART	ARTS	DHA	-	ART	ARTS	DHA	-	ART	ARTS	DHA
CH_2/CH_3	4.51 ±2.15	4.81 ±2.02	4.56 ±1.01	4.33 ±2.62	0.90 ±0.15	1.25 ±0.33	1.24 ±0.77	0.90 ±0.19	2.87 ±0.89	2.37 ±0.06	2.44 ±0.18	2.69 ±0.03	3.62 ±1.42	3.14 ±0.25	2.92 ±0.48	3.20 ±0.02
Glutamate / Lactate	2.61 ±0.86	0.88* ±0.19	1.26** ±0.38	1.11** ±0.36	0.74 ±0.14	0.90 ±0.04	0.85 ±0.01	0.85 ±0.21	1.31 ±0.16	1.05 ±0.47	1.54 ±0.31	0.85** ±0.03	0.73 ±0.03	1.46* ±0.1	1.50* ±0.01	1.67* ±0.19
Aspartate / Lactate	0.37 ±0.07	0.32 ±0.15	0.53 ±0.17	2.21* ±0.03	0.56 ±0.17	0.94** ±0.21	1.24** ±0.4	1.25* ±0.29	2.74 ±1.17	2.54 ±0.07	2.43 ±0.26	2.21 ±1.8	1.09 ±0.23	3.82* ±0.19	3.35** ±0.74	3.93** ±1.14

Presented are mean values and their standard deviations (SD) for each cell line and each qinghaosu after 2h treatment. The effects of treatments on K562, GLC4, K562/*adr* and GlC4/*adr*cells were compared to control untreated cells by independent t–test.

* significantly different from control , $P < 0.05$

** significantly different from control, $P < 0.10$

*** significantly different from control, $P < 0.15$

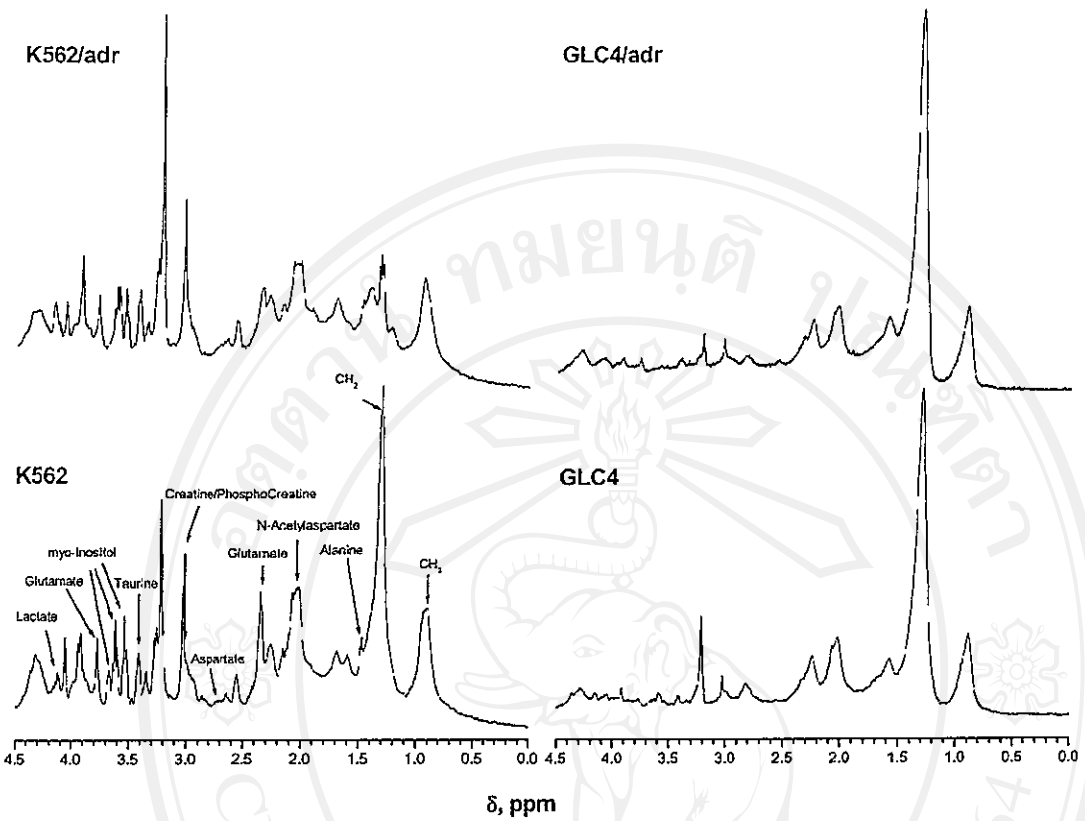

Figure 1. ^{1}H–NMR spectra obtained from K562, GLC4, K562/*adr* and GlC4/*adr* cells. Cells (10^6 cells/mL) for 10 mL were incubated in the absence for 2 h at 37°C, centrifuge at 1800 rpm for 10 minutes. The pellets were rinsed twice using PBS and three times washed using PBS/D_2O. The cells were counted using hematocytometer and were loaded into a 5–mm Shigemi NMR tube, completed with 450 mL PBS/D_2O.

b) ^{1}H-NMR spectra of treated cells: in order to visualize the changes in metabolites after exposing to these cytotoxic drugs, cells were incubated in the presence of 30 μM artemisinin, artesunate or dihydroartemisinin for 2 h at 37 °C, then the ^{1}H–NMR spectra were registered and analyzed as indicated in Table 1. All compounds stimulate a decrease in lactate production of K562 cells and only dihydroartemisinin stimulates an increase in aspartate of K562 cell but no significant changes were observed in those of GLC4 cells. The lactate was found to decrease in both of drug-resistant cells when compared with the control series; K562/*adr* from 0.59 ± 0.04 to 0.30 ± 0.03 for artemisinin (P<0.05), from 0.59 ± 0.17 to 0.28 ± 0.12 for artesunate (P<0.1) and from 0.59 ± 0.17 to 0.28 ± 0.12 for dihydro-artemisinin (P<0.05); GLC4/*adr* from 0.68 ± 0.15 to 0.32 ± 0.04 for artemisinin (P<0.1), from 0.68 ± 0.15 to 0.33 ± 0.11 for artesunate (P<0.1) and from 0.68 ± 0.15 to 0.25 ± 0.06 for dihydroartemisinin (P<0.1). In particular, a decrease in lactate with

accompanied by an increase in aspartate was determined only in GLC4/*adr* cells; from 0.73 to 1.21 ± 0.09 for artemisinin ($P<0.01$), from 0.73 to 1.05 ± 0.13 for artesunate ($P<0.1$) and from 0.73 to 0.96 ± 0.04 for dihydroartemisinin ($P<0.05$). The decline in glutamate was found with out any significant change in aspartate was found in K562/adr cells. No significant changes in taurine and myo-inositol were found.

The mobile lipids (ML) representing saturated lipids, $-CH_2$ (δ = 1.3 ppm) and $-CH_3$ (δ = 0.9 ppm) groups and creatine/phosphocreatine (δ = 3.05 ppm) were assigned as indicated in Figure 1. Table 2 shows the ratios of $-CH_2/-CH_3$ obtained from untreated and treated cells using 30 μM drugs for 2h. The ratios of $-CH_2/-CH_3$ was considered as an indicator reflects an irreversible cellular damage accompanying apoptosis. No significant change in mobile lipid profiles before and after treating series were found.

3.2 Determination of apoptosis by using flow cytometer

A typical result of apoptosis–inducing activity of dihydroartemisinin performed in GLC4/adr cells was shown Figure 2. However, dihydroartemisinin significantly caused cell death via necrosis which can be found at 24 and 72h after treatment. The biparametric plots demonstrated that dihydroartemisinin exhibited an apoptosis-inducing activity as time– and concentration– dependent manner (Figure 3). The percentage of apoptosis obtained from the series of experiments using 15 μM dihydroartemisinin in K562, K562/*adr*, GLC4 and GLC4/*adr* cells was increased ranging from 5 ± 2 % to 18 ± 5 % when the incubation time increased from 6 h to 72 h (Figure 3a). The percentage of apoptosis obtained from the series of experiments using variation of dihydroartemisinin concentration at 24 h after treatment was shown in Figure 3b which indicated the maximal apoptosis–inducing effects was about 20%. The drugs used in this study exhibited similar apoptosis-inducing activity in the four cell lines as indicated in Figure 3c. The same direction of results but lesser efficacy than dihydroartemisinin were found when the same conditions, experiments were performed using artemisinin and artesunate.

3.3 Determination of intracellular pH and intraluminal of lysosomal pH

In order to verify that artemisinin, artesunate and dihydroartemisinin induced changes in the cellular glucose metabolism might affect intracellular pH regulation. The intracellular pH and intraluminal of lysosomal pH was monitored using arcidine orange by monitoring the red and green fluorescence which reflect the amount of acridine orange accumulated at lysosomes and at cytoplasm of cells.

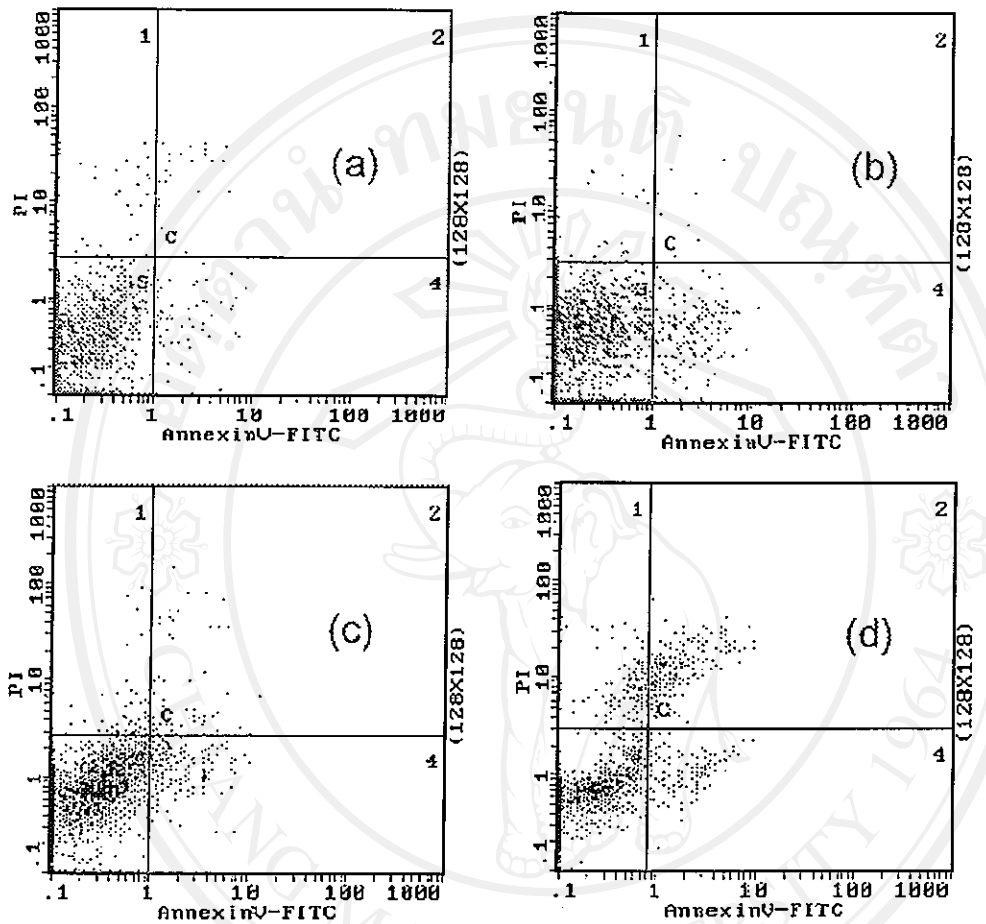

Figure 2. Representative biparametric histrogram of an Annexin V–FITC versus PI of GLC4/*adr* cells; (a) untreated and after (b) 6 h, (c) 24 h and (d) 72 h treatement using 15 μM dihydroartemisinin before staining as described in materials and methods).

As can be expected, the green fluorescence significantly increases but no significant change of red fluorescence in the treated series compared with control series. Figure 4 show that the ratios of red/green fluorescence decrease by 40% and 55% in drug-sensitive and drug-resistant cells, respectively. These results suggest an acidified of intracellular pH of the two cell lines .

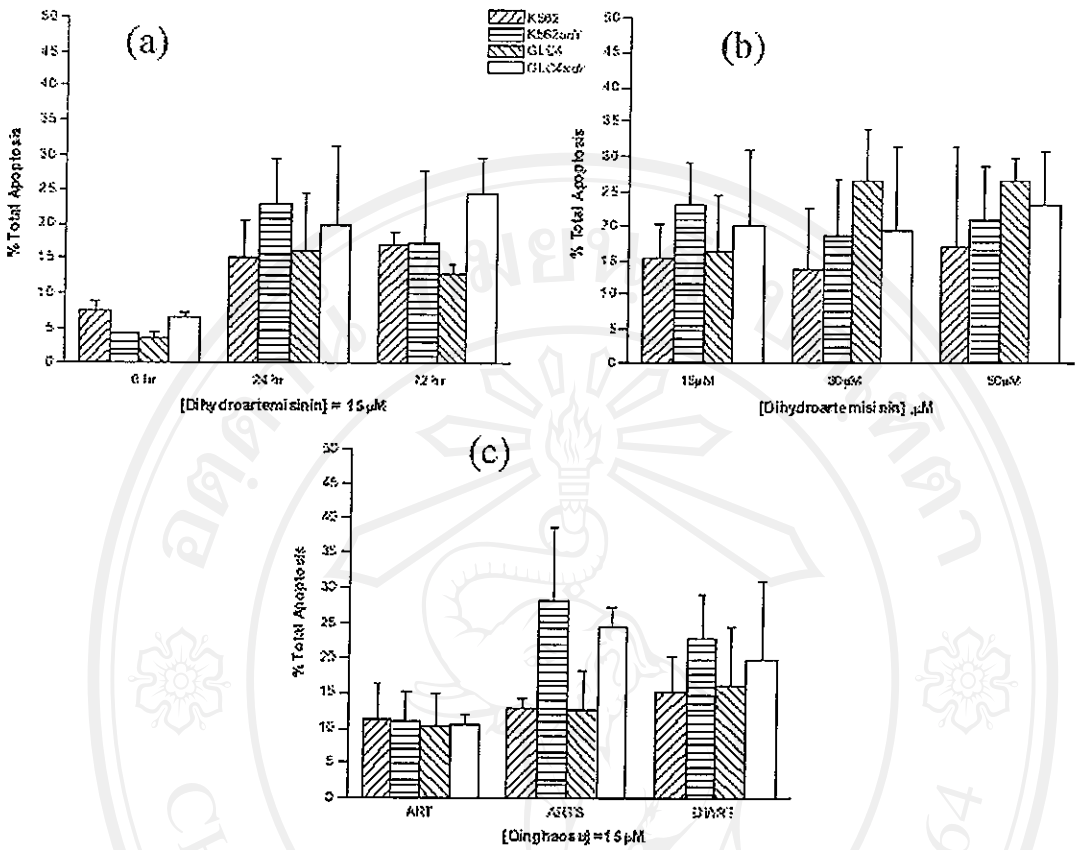

Figure 3. Apoptosis–inducing activity of dihydroartemisinin against K562, GLC4, K562/*adr* and GlC4/*adr* cells. The total apopotosis presents as a function of (a) time– and (b) concentrations. (c) Apoptosis–inducing activity of 15 μM drugs against K562, GLC4, K562/*adr* and GlC4/*adr* cells.
– Cells were exposed to dihydroartemisinin with varied concentration and times as indicted in the figure before staining using Annexin V–FITC and PI. Flow cytometry analysis was performed in a Coulter Epics XL–MCL^{TM} and cells were evaluated on 5000 events per sample. Each value is represented as the mean± S.D. of three independent experiments. ($P< 0.05$)

4. DISCUSSION

In the present study demonstrates that the changes in glucose catabolic biomarkers of cells exposed to artemisinin, artesunate and dihydro-artemisinin can be monitored by ^{1}H-NMR spectroscopy. In particular, the presence of lactate and both of glutamate and aspartate that correspond to the anaerobic and oxidative metabolic, respectively and these metabolic products can be used as indicators for studying cellular energy production. On the basis of ^{1}H-NMR finding, since glutamate was found 2.61 ± 0.8 fold for K562 and 1.31 ± 0.16 fold for GLC4 cells higher than lactate signifies that both of drug–sensitive cells produce energy via

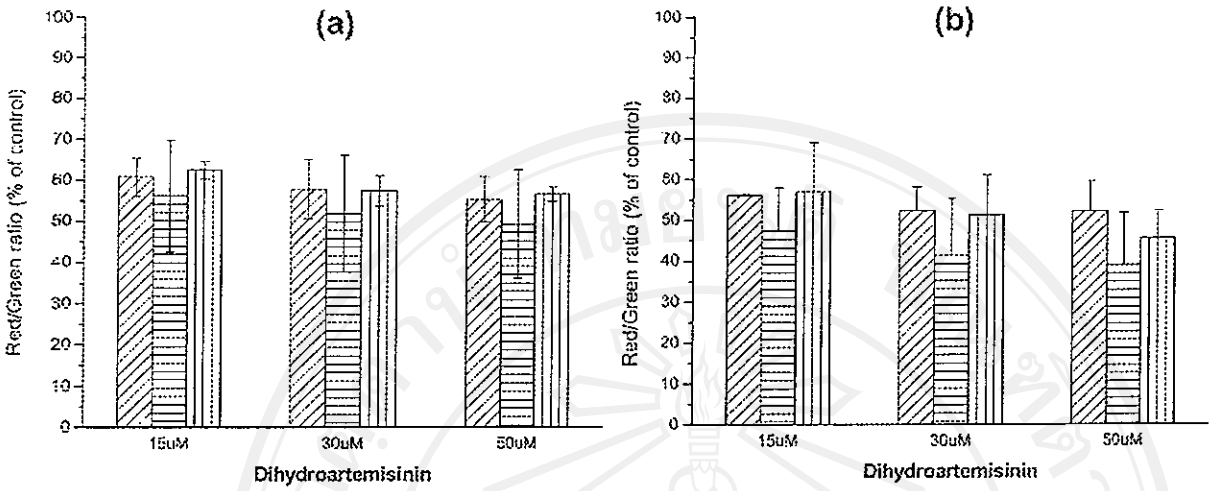

Figure 4. Changes in ratios of red to green fluorescence after 24 h (▨), 48 h (▤) and 72 h (▥) treatment using indicated concentration of dihydroartemisinin in (a) K562 and (b) K562/adr cells. Each value is represented as the mean ± S.D. of three independent experiments. ($P< 0.05$)

oxidative metabolism. However, the two drug-sensitive cells produce the lactate in high amounts, particularly GLC4 two–fold higher than K562 cells ($P<0.01$), indicating that these cells can maintain an increased rate of glucose utilization and sustain high rates of glycolysis. The rate of glucose utilization via glycolysis significant increases when the similar series of experiments were performed using their corresponding drug-resistant cells. The ratios of glutamate to lactate was equal to 0.74 ± 0.14 for K562/adr and 0.73 ± 0.03 for GLC4 cells where no–significant difference of lactate was found in both MDR cells (lactate = 0.59 ± 0.17 for K562/adr and 0.68 ± 0.15 for GLC4/adr, $P<0.56$). Both drug-resistant cells significantly produce lactate higher than K562 cells ($P< 0.01$) but no-significant difference to GLC4 ($P < 0.16$). The results also suggest that particularly in drug-resistant cells, there is an up-regulation of a derive energy supplies by glycolysis pathway and this become more important than oxidative metabolism sine the ratios of glutamate to lactate are lower than 1.

^{1}H–NMR spectra obtained from the treatment series revealed that artemisinin, artesunate and dihydro-artemisinin affected the metabolism of these cell lines. In drug–sensitive cells, they inhibit the oxidative metabolism study however; GLC4 cells show low sensitivity to the drugs. In drug-resistant cells, the drugs inhibit the anaerobic but stimulate the oxidative metabolic of these MDR cells. These should be resulted in a decrease in global cellular ATP contents which consistency our previous reports (Reungpatthanaphong *et al.*, 2002). However, an abnormal oxidative metabolism was observed in K562/adr cells; as a decrease in glutamate is not accompanied by any increase in aspartate, signifies that an abnormal mitochondrial function of the cells,

probably the original of a lower mitochondrial energetic state which can be measured by the $\Delta\Psi m$ compared with K562 cells (Reungpatthanaphong *et al.*, 2003). These results suggest that altered mitochondrial dynamics is nonrandom in MDR cells; thus, the mitochondria may be involved in the production of a pleiotropic MDR phenotype. It was proposed that rapid overexpression of MDR1/P–glycoprotein is associated with a decrease of $\Delta\Psi m$ (Shtil *et al.*, 2000). An increase or a decrease in $\Delta\Psi m$ consequently followed an increase or a decrease in cellular ATP content. We have found that an increase in cellular ATP content in MDR cells via oxidative phosphorylation can protect cells from toxicity induced by pirarubicin. This probably assures the function of the P–glycoprotein and MRP1 protein (Reungpatthanaphong *et al.*, 2003). The origin of ATP synthesis, such as the mitochondria, can be used as a specific target for MDR modulator research.

We have also previously reported that artemisinin, artesunate and dihydroartemisinin exhibit anticancer activity in micro molar concentration range and have 2-fold more efficacies in K562/*adr* and GLC4/*adr* than their corresponding drug-sensitive cells (Reungpatthanaphong & Mankhetkorn, 2002). The results present herein demonstrate that at lower to 15 μM, even through cells were exposed to drugs varied from 0 to 72 h, and only 3 % total apoptosis were determined. These are along with the ^{1}H–NMR studies which found that no significant changes of mobile lipids. The significant apoptosis-inducing activity of drugs were found when the concentrations used are higher than 15 μM and the maximal apoptosis–inducing activity was about 20% even the concentration of drugs increase up to 50 μM.

In conclusion artemisinin, artesunate and dihydroartemisinin stimulate a decrease in oxidative metabolic of both drug–sensitive cells while increase in the efficacy of oxidative metabolic of both drug-resistant cells lines. These were accompanied by an intracellular acidification and an induction of both necrosis and apoptosis. ^{1}H–NMR spectroscopy can be used to simultaneously monitor the lactate, glutamate and aspartate as indicators for studying cellular production of energy.

ACKNOWLEDGEMENT

Reungpatthanaphong P. thank for the Royal Golden Jubilee Ph.D. program for their financial support.

REFERENCES

Benakis, A., Paris, M., Loutan, L., Plessas, C.T. & Plessas, S.T. (1997). Pharmacokinetics of artemisinin and artesunate after oral administration in healthy volunteers. *The American Journal of Tropical Medicine and Hygiene*, 56, 117–123.

Chen, H.H., You, L.L. & Shi, M.F. (2004). Artesunate inhibits angiogenesis and induces apoptosis in human umbilical vein endothelial cell. *Pharmacological Research*, (In press).

Efferth, T., Dunstan, H., Sauerbrey, A., Miyachi, H. & Chitambar, C.R. (2001). The antimalarial artesunate is also active against cancer. *International Journal of Oncology*, 18, 767–773.

Efferth, T., Davey, M., Olbrich, A., Rücher, G., Gebbart, E. & Daveu, R. (2002). Activity of drugs from

traditional Chinese medicine toward sensitive and MDR1- or MRP1-overexpressing multidrug-resistant human CCRF-CEM leukemia cells. *Blood Cells, Molecules & Diseases*, 28, 160–168.

Hien, T.T. & White, N.J. (1993). Qinghaosu. *Lancet*, 6(341), 603–608.

Klayman, D.L. (1985). Qinghaosu (artemisinin): an antimalarial drug from China. *Science*, 31(228), 1049–1055.

Kothan, S., Dechsupa, S., Leger, G., Moretti, J.L., Vergote, J., Mankhetkorn, S. (2004). Spontaneous mitochondrial membrane potential change during apoptotic induction by quercetin in K562 and K562/adr cells. *Canadian Journal of Physiology and Pharmacology*, 82, 1084–1090.

Lozio, C. B. & Lozio, B. B. (1975). Human chronic myelogenous leukemia cell–line with positive Philadelphia chromosome. *Blood*, 45, 321–334.

Mankhetkorn, S., Teodori, E., Scapecchi, S. & Garnier–Suillerot, A. (1996) Study of P–glycoprotein functionality in living resistant K562 cells after photolabeling with a verapamil analogue. *Biochemical Pharmacology*, 52, 213–217.

Mannechez, A., Reungpatthanaphong, P., de Certaines, J.D., Leray, G. & Moyec, L.L. (2005). Proton NMR visible mobile lipid signals in sensitive and multidrug-resistant K562 cells are modulated by rafts. *Cancer Cell International*, 5, 1–10.

Miccheli, A., Tomassini, A., Puccetti, C., Valerio, M., Peluso, G., Tuccillo, F., Calvani, M., Manetti, C. & Conti, F. (2005). Metabolic profiling by ^{13}C–NMR spectroscopy: [1,2-$^{13}C_2$] glucose reveals a heterogeneous metabolism in human leukemia T cells. *Biochimie*, In Press

Muller, M., Meijer, C., Zaman, G. J. R., Borst, P., Scheper, R. J., Mulder, N. H., de Vries, E. G. E. & Jansen, P. L. M. (1994). Overexpression of the gene encoding the multidrug resistance–associated protein results in increased ATP–dependent glutathione S–conjugate transport. *Proceedings of the National Academy of Sciences of the United States of America*, 91, 13033–13037.

Papas, K.K., Colton, C.K., Gounarides, J.S., Roos, E.S., Jarema, M.A., Cheng, M.J., Shapiro, L.L., Cline, G.W., Shulman, G.I., Wu, H., Bonner-Weir, S. & Weir, G.C. (2001). NMR spectroscopy in beta cell engineering and islet transplantation. *Annals of the New York Academy of Sciences*, 944, 96–119.

Pfeuffer, J., Tkac, I., Provencher, S.W. & Gruetter, R. (1999). Toward an in vivo neuro-chemical profile: quantification of 18 metabolites in short-echotime (1)H NMR spectra of the rat brain. *Journal of Magnetic Resonance*, 1, 104–120.

Pfeuffer, P., Joseph, C. L., Lance, D.B, Kamil, U. & Michael, G. (2005). Detection of intracellular lactate with localized diffusion {^1H–^{13}C}–spectroscopy in rat glioma in vivo. *Journal of Magnetic Resonance*, 177, 129–138.

Reungpatthanaphong, P. & Mankhetkorn, S. (2002). Modulation of Multidrug Resistance by Artemisinin, artesunate and dihydro-

artemisinin in K562/*adr* and GLC4/*adr* Resistant Cell Lines. *Biological & Pharmaceutical Bulletin*, 25, 1555–1561.

Reungpatthanaphong, P., Dechsupa, S., Meesungnoen, J., Loetchutinat, C.& Mankhetkorn, S. (2003). Rhodamine B as a mitochondrial probe for measurement and monitoring of mitochondrial membrane potential in drug–sensitive and –resistant cells. *Journal of Biochemical and Biophysical Methods*, 57, 1–16.

Sharma, U., Mehta A., Seenu V. & Jagannathan N.R. (2004). Biochemical characterization of metastatic lymph nodes of breast cancer patients by in vitro 1H magnetic resonance spectroscopy: a pilot study. *Magnetic Resonance Imaging*, 22(5), 697–706.

Shtil, A.A., Grinchuk, T.M., Tee, L., Mechetner, E.B. & Ignatova, T.N. (2000). Overexpression of P–glycoprotein is associated with a decreased mitochondrial transmembrane potential in doxorubicin–selected K562 human leukemia cells. *International journal of oncology*, 17, 387–397.

Singh, N.P. & Lai, H. (2001). Selective toxicity of dihydroartemisinin and holotransferrin toward human breast cancer cells. *Life Sciences*, 70(1), 49–56.

Singh, N. P. & Verma, K.B. (2002). Case report of a laryngeal squamous cell carcinoma treated with artesunate. *Archives of Oncology*, 10, 279–280.

Sunil, K., Ziad, R., Doris, M. J., France, B., Andreas, F. & Laurent, B.F. (2006). Probing gender–specific metabolism differences in humans by nuclear magnetic resonance–based metabonomics. *Analytical Biochemistry*, In Press

Tsuro, T., Iida, H., Kawabata, H., Oh-Hara, T., Hamada, H. & Utakoji, T. (1986). Characteristics of resistance to adriamycin in human myelogenous leukemia K562 resistant to adriamycin and in isolated clones. *Japanese Journal of Cancer Research*, 77, 682–692.

Versantvoort, C.H.M., Withoff, S., Broxterman, H.J., Kuiper, C.M., Scheper, R.J., Mulder, N.H., de Vries, E.G.E. (1995). Resistance-associated factors in human small–cell lung–carcinoma GLC4 sublines with increasing adriamycin resistance. *International Journal of Cancer*, 61, 375–380

Woerdenbag, H.J., Moskal, T.A., Pras, N., Malingre, T.M., el-Feraiy, F.S., Kampinga, H.H. & Konings, A.W. (1993). Cytotoxicity of artemisinin–related endoperoxides to Enrlich ascites tumor cells. *Journal of Natural Products*, 56, 849–856.